RSC Advances

ROYAL SOCIETY OF CHEMISTRY

www.rsc.org/advances

Graphical abstract image

This work reported the fabrication of amphiphilic TPEV-PEG fluorescent copolymers *via* RAFT polymerization of polymerizable AIE and PEGMA with promising applications for bioimaging.

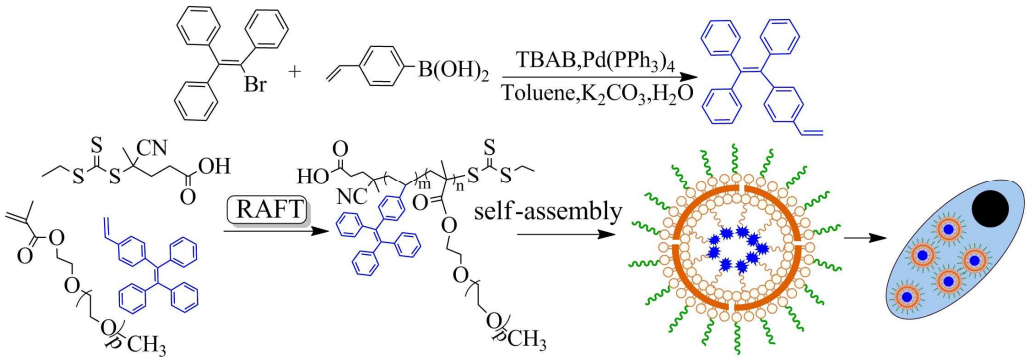

Cite this: DOI: 10.1039/c0xx00000x

www.rsc.org/xxxxxx

PAPER

Synthesis of amphiphilic fluorescent PEGylation AIE nanoparticles *via* RAFT polymerization and their cell imaging applications

Zengfang Huang,*[a,b] Xiqi Zhang,[b,c] Xiaoyong Zhang,[b] Shiqi Wang,[b] Bin Yang,[b] Ke Wang,[b] Jinying Yuan,[b] Lei Tao*[b] and Yen Wei*[b]

Received (in XXX, XXX) Xth XXXXXXXXX 20XX, Accepted Xth XXXXXXXXX 20XX
DOI: 10.1039/b000000x

With the increasing interest of luminescent probes in biomedical applications, the development of fluorescent organic nanoparticles (FONs) on the basis of aggregation induced emission (AIE) dyes was attracting people's great research attention. In this study, a polymerizable tetraphenylethene-functionalized AIE dye (named as TPEV) with a vinyl end functional group was synthesized by "one-step" Suzuki coupling reaction of 4-vinylphenylboronic acid and bromotriphenylethylene, and the as-prepared hydrophobic AIE dye TPEV subsequently participated in the reversible addition-fragmentation chain transfer (RAFT) polymerization together with the hydrophilic monomer of poly(ethylene glycol) monomethacrylate (PEGMA) to obtain a new amphiphilic copolymer (denoted as TPEV-PEG) with transformed side fluorescent groups. The M_n value of the obtained copolymer was about 29800 g mol^{-1} with a narrow polydispersity index (PDI) as about 1.30. The molar ratio of TPE to PEG segment in the copolymer was respectively about 19.2% to 80.8%, and it was easy for the TPEV-PEG copolymer to self-assemble into FONs with the hydrophobic AIE core encapsulated by hydrophilic PEG shell. The research results further exhibited that the TPEV-PEG FONs presented good fluorescent feature with the maximal emission peak at 480 nm, high dispersibility in water solution with homogeneous spherical morphology (~200 nm) and excellent biocompatibility, making them highly potential for bioimaging applications.

1. Introduction

As a metal-free approach, RAFT polymerization has the excellent tolerance to many functional monomers and numerous solvents, which has been regarded as a powerful tool to facilely fabricate numerous functional polymers with anticipant molecular weights and architectures with narrow polydispersity index (PDI).[1-7] Recently, our group reported a one-pot combination of RAFT polymerization and transesterification of 2,2,2-trifluoethyl methacrylate (TFEMA) with *n*-hexanol, and the kinetic indicated that the molecular weight increased linearly with monomer conversions and the polymerization had the characteristics of a controllable polymerization.[8] Another novel 'one pot' KF-RAFT strategy was successfully developed by combining an effective KF reaction and RAFT process, and it is facile and efficient for this system to obtain new side functionalized poly(aminophosphonate)s (polyAPPs).[9] Moreover, RAFT polymerization method was also adopted to prepare AIE copolymers. Taking EDMAT and AIBN as the free chain transfer agent and the radical initiator, the AIE copolymer of styrene or 4-vinylpyridine was successfully prepared, subsequently, the block amphiphilic AIE copolymer was further obtained by the reaction of polyvinylpyridine copolymer with an excess amount of iodomethane in DMSO.[10] A red cross-linkable R-PEG FONs *via* RAFT polymerization of cross-linkable AIE dye (R-E) and PEGMA were reported in our previous work.[11] Without catalysts or initiators, a novel technique for preparing $PhNH_2$-OA-PEG FONs has been further investigated *via* one-pot combination of ring-opening polymerization and condensation reaction at room temperature and in air.[12-13] These as-prepared FONs showed strong fluorescence, high water dispersibility, and excellent biocompatibility, which were promising for applications in bioimaging field.

Recently, the development of FONs based on AIE dyes has attracted great research attention.[14] Due to scientists' enthusiastic investigation, a large variety of AIE molecules have been developed with great structural variety, and a few typical examples were as tetraphenylethene (TPE), hexaphenylsilole (HPS) and distyreneanthracene (DSA).[15-17] Among these AIE molecules, TPE derivative is a class of widely known AIE material, which has been expansively developed for chemosensor and biomedical applications.[18-20] Although small molecular AIE dyes have acquired great progress, polymers and other macromolecules on the basis of AIE molecules have been less explored.[21] As compared with small molecules, polymer materials have many advantages, such as various opportunities to adjust the structure, topology and morphology, as well as easy functionalities.[22] Therefore, polymerization with AIE dye provides a much larger platform for material operation. For

[a]*College of Chemistry and Biology，Zhongshan Institute, University of Electronic Science & Technology of China，Zhongshan, 528402, P. R. China. hzf105@163.com*
[b]*Department of Chemistry, the Tsinghua Center for Frontier Polymer Research, Tsinghua University, Beijing 100084, P. R. China. E-mail: leitao@mail.tsinghua.edu.cn; weiyen@tsinghua.edu.cn*
[c]*Laboratory of Bio-Inspired Smart Interface Science, Technical Institute of Physics and Chemistry, Chinese Academy of Sciences, Beijing, 100190, P. R. China.*

example, a poly(N-isopropylacrylamide) (PNIPAM) with a TPE fluorogen segment was acquired by direct copolymerization of N-isopropylacrylamide and monomer containing TPE segment *via* AIBN-initiated free radical polymerization. Thus, it is effective for incorporating a small amount of AIEgen to convert PNIPAM into an AIE polymer while keeping the original characteristics of PNIPAM.[23] In another work, the partially substituted polymer of poly(acrylic acid) (PAA) was obtained *via* amidation of amino-containing TPE derivative linked onto PAA. The acid functional groups and hydrophobic TPE pendants respectively made the polymer have pH-responsiveness and AIE features.[17] The linear polymer with TPE building blocks was facilely generated by Suzuki coupling polymerization of TPE-containing dibromide and diboronic acid, and the as-prepared polymer had high thermal stability and AIE-active feature by the rigid structure and TPE segment.[24] TPE-containing diacrylates were polymerized using AIBN as an initiator in refluxing THF under mild reaction conditions, and the addition of a small amount of water into the THF solution would make the fluorescence of the obtained polymer increase obviously.[25] Our group facilely prepared TPE-based AIE FONs with stable C-N covalent bond *via* Schiff base condensation with ε-polylysine (Ply).[26] Another one-pot strategy for the fabrication of TPE-based FONs was developed *via* combination of RAFT polymerization and transesterification reaction, and the molar fraction of TPE and PEG in the polymer was about 30.5% and 69.5%. These FONs presented spherical morphology, uniform size, and excellent biocompatibility.[27]

It was a powerful and convenient strategy for RAFT polymerization of polymerizable AIE monomer combining with some hydrophilic monomer to fabricate the amphiphilic AIE copolymer, which will tend to self-assemble into FONs, making them promising for bioimaging applications. In this contribution, a polymerizable AIE dye of tetraphenylethene-functionalized monomer (TPEV) was synthesized by Suzuki coupling reaction of 4-vinylphenylboronic acid and bromotriphenylethylene, which subsequently participated in the RAFT polymerization with the hydrophilic monomer of PEGMA to obtain a new amphiphilic AIE copolymer (TPEV-PEG) with transformed side fluorescent groups. The obtained TPEV-PEG copolymer tended to self-assemble into FONs in aqueous solution. To study the cell imaging application, the dispersibility, AIE property, and biocompatibility of TPEV-PEG FONs were further investigated.

2. Experimental

2.1. Materials and characterization

Poly(ethylene glycol) monomethacrylate (PEGMA, M_n = 500, J&K Chemical, AR), 2,2'-azobisisoheptonitrile (AVBN, J&K Chemical, 98%), tetrakis(triphenylphosphine)palladium(0) ($Pd(PPh_3)_4$, J&K Chemical, 97%), 4-vinylphenylboronic acid (J&K Chemical, 97%), bromotriphenylethylene (J&K Chemical, 95%), tetrabutyl ammonium bromide (TBAB, J&K Chemical, 98%), and triethylamine (TEA, J&K Chemical, AR) were all used as purchased. The chain transfer agent (CTA) of 4-cyano-4-(ethylthiocarbonothioylthio) pentanoic acid were synthesized by reference to the literature methods.[28]

Gel permeation chromatography (GPC) analysis of the TPEV-PEG copolymer was performed on a CBM-20A at room temperature based on standard polystyrene as the reference with N,N-dimethyl formamide (DMF) as the solvent. ^{1}H-NMR spectra of TPEV dye and its TPEV-PEG copolymer were carried out on a JEOL JNM-ECA 400 (400 MHz) spectrometer at room temperature in a $CDCl_3$ solution with tetramethylsilane (TMS) as a reference. Elemental analysis (EA) of TPEV dye was performed on an Elementar Vario EL elemental analyzer. The transmission electron microscopy (TEM) specimen was made by placing a drop of the TPEV-PEG suspension on a carbon-coated copper grid, and TEM image was recorded on a JEM-1200EX microscope operated at 100 kV. UV-vis absorption spectrum of TPEV-PEG copolymer was performed on a Perkin-Elmer LAMBDA 35 UV-vis system. Fluorescence emission (FL) spectra of TPEV-PEG in water or THF solution were measured on a PE LS-55 spectrometer. The FT-IR spectra of TPEV dye and TPEV-PEG copolymer were obtained in a reflection mode on a Perkin-Elmer Spectrum 100 spectrometer (Waltham, MA, USA).

2.2. Synthesis of tetraphenylethene-functionalized vinyl (TPEV)

The synthesis of the fluorescent TPEV dye was as follows: Bromotriphenylethylene (1.05 g, 3.13 mmol) and 4-vinylphenylboronic acid (0.56 g, 3.75 mmol) were dissolved in the mixture of toluene (22 mL), TBAB (0.10 g, 0.31 mmol) and 2 M potassium carbonate aqueous solution (5.6 mL). The mixture was stirred at room temperature for 0.5 h under N_2 gas followed adding $Pd(PPh_3)_4$ (4.2 mg, 3.65×10^{-3} mmol) and then heated to 90 °C for 24 h. Subsequently, the mixture was poured into water and extracted three times with ethyl acetate. The organic layer was dried over anhydrous sodium sulfate. After removing the solvent under vacuum, the residue was chromatographed on a silica gel column with *n*-hexane/CH_2Cl_2 (2:1 by volume) as eluent to give TPEV (0.85 g, 76% yield). ^{1}H NMR (400 MHz, $CDCl_3$, δ): 5.17 (d, *J*=8.0 Hz, 1H; CH), 5.66 (d, *J*=12.0 Hz, 1H; CH), 6.61 (t, *J*= 8.0 Hz, 1H; CH), 6.96-7.15 (m, 19H; Ar H); ^{13}C NMR (100 MHz, $CDCl_3$, δ): 113.56, 125.62, 126.50, 126.56, 127.71, 127.84, 131.43, 131.62, 135.58, 136.66, 140.65, 141.12, 143.43, 143.79; Anal. calcd for $C_{28}H_{22}$: C 93.81, H 6.19; found: C 93.69, H 6.31.

2.3. Synthesis of fluorescent copolymer (TPEV-PEG)

The fabrication of the fluorescent copolymer TPEV-PEG was as follows: TPEV (50 mg, 0.140 mmol), PEGMA (310 mg, 0.620 mmol), CTA (2.8 mg, 1.06×10^{-2} mmol), AVBN (1.3 mg, 0.524×10^{-2} mmol) and 1.0 mL toluene solvent were added into a Schlenk tube consisting of a magnetic stir bar, and then followed by freeze-pump-thaw circle with nitrogen three times. The Schlenk tube was introduced into an oil bath kept at 55 °C for 30 h. Finally, the mixed solvent was removed under vacuum. The copolymer was further purified by precipitation from THF to petroleum ether for three times, and then dried under vacuum for characterization and cell imaging applications. yield: 0.30 g. Finally, 10 mg TPEV-PEG copolymer was added to 5 mL H_2O, then shaken until it had been dissolved completely, which was used to investigated its self-assembly in H_2O solution.

2.4. Cytotoxicity of TPEV-PEG FONs

The observation of cell morphology was used to investigate the effects of TPEV-PEG FONs on HepG2 cells.[29] Briefly, cells were seeded into 6-well microplates in 2 mL of respective media at a

density of 1×10^5 cells mL^{-1} containing 10% fetal bovine serum (FBS). After cell attachment, plates were washed with PBS and cells were treated with complete cell culture medium, or different concentrations of TPEV-PEG FONs prepared in 10% FBS containing media for 24 h. Then all samples were washed with PBS three times to remove the uninternalized FONs. An optical microscopy (Leica, Germany) was used to observe the morphology of cells, whose overall magnification was ×100.

The cell counting kit-8 (CCK-8) assay was used to examine the cell viability of TPEV-PEG FONs on HepG2 cells on the basis of our previous reports. In brief, cells were seeded in 96-well microplates at a density of 5×10^4 cells mL^{-1} in 160 μL of respective media containing 10% FBS. After cell attachment for 24 h, the cells were incubated with 10, 20, 40, 80, 120 μg mL^{-1} TPEV-PEG for 8 and 24 h, and then the cells were washed with PBS three times to remove the uninternalized TPEV-PEG FONs. 10 μL of CCK-8 dye and 100 μL of DMEM cell culture medium were added into each well and incubated for 2 h at 37 °C. Finally, the plates were analyzed with a microplate reader (Victor III, Perkin-Elmer). The absorbance of formazan dye was obtained at 450 nm, with 620 nm as the reference wavelength. The absorbance values were proportional to the number of live cells. The percent reduction of CCK-8 dye was obtained taking controls (cells not exposure to TPEV-PEG FONs) as the reference, which represented 100% CCK-8 reduction. The microplate experiment was repeated three times with three replicate wells. Cell survival was expressed as absorbance relative to that of untreated controls, and the results are presented as mean ± standard deviation (SD).

2.5. Confocal microscopic imaging of cells using TPEV-PEG FONs

The cell uptake of TPEV-PEG FONs was further evaluated by the confocal microscopic imaging.[27, 30] Briefly, cells were seeded in a glass bottom dish with a density of 1×10^5 cells per dish. On the day of treatment, the cells were incubated with TPEV-PEG FONs at a final concentration of 80 μg mL^{-1} for 3 h at 37 °C. Afterwards, the cells were washed three times with PBS to remove the TPEV-PEG FONs and then fixed with 4% paraformaldehyde for 10 min at room temperature. Cell images were obtained by confocal laser scanning microscope Zeiss 710 3-channels (Zeiss, Germany) with 405 nm as the excitation wavelength.

3. Results and discussion

Previously, a polymerizable tetraphenylethene-functionalized AIE dye was successfully synthesized by "three-steps" method: synthesis of 1-(4-bromophenyl)-1,2,2-triphenylethylene (1), formolation of (1) and the Wittig reaction of (2) affording vinyl tetraphenylethylene dye.[31] Herein, the TPEV dye was synthesized by "one-step" Suzuki coupling reaction of 4-vinylphenylboronic acid and bromotriphenylethylene with high yield insteading of the above "three-steps" method,[18] which subsequently copolymerized with the hydrophilic monomer of PEGMA to produce new amphiphilic fluorescent copolymers with transformed side fluorescent groups *via* RAFT polymerization. The obtained TPEV-PEG copolymers would have excellent fluorescence by the introduction of TPEV dye; moreover, hydrophilic PEG chain would also endow them with the good water solubility. It was expected for the obtained amphiphilic fluorescent copolymers to be self-assembled into nanoparticles and further internalized by cell. The synthetic procedure in this report was schematically displayed in Scheme 1.

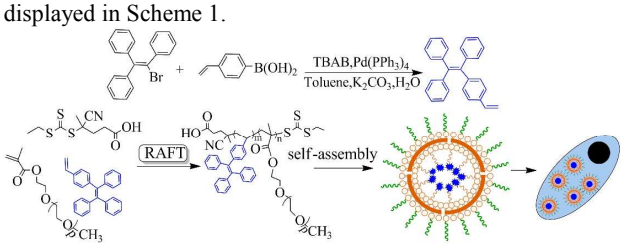

Scheme 1. Schematic showing synthesis of TPEV fluorescent dye and its TPEV-PEG copolymer through RAFT polymerization, and then self-assembly of these copolymer for cell imaging.

Fig. 1A describes the number average molecular weight (M_n) and the PDI of the final obtained TPEV-PEG copolymers, which were respectively about 29800 g mol^{-1} and 1.30. The structure of the TPEV dye and TPEV-PEG copolymers was analyzed by ^1H NMR spectra as exhibited in Fig. 1B. For TPEV spectrum, the phenyl hydrogen peaks of TPEV appear clearly at the range of 6.96-7.25 ppm, and the characteristic peaks of polymerizable CH_2=CH- group can be clearly observed at 5.19, 5.68, and 6.62 ppm, the integral ratio of which is 1:1:1, confirming the successful synthesis of TPEV dye. For TPEV-PEG copolymers spectrum, the characteristic peaks of CH_2=CH- group have disappeared, and the phenyl hydrogen peaks of TPEV segment are clearly observed at the range of 6.96-7.10 ppm with the characteristic peak of ester group linked to acrylate of the PEGMA at 4.05 ppm,[27] and the peaks at 3.63 ppm and 3.36 ppm should be the other ester groups of PEG segment and $-CH_3$ at PEGMA end, indicating the successful incorporation of both TPEV and PEGMA into the copolymers via RAFT polymerization. Referring to the integral area ratio of the peaks at 6.96-7.10 ppm and 4.05 ppm, the respective molar fraction of TPEV segment and PEG segment in the copolymers was calculated as about 19.2% and 80.8%.

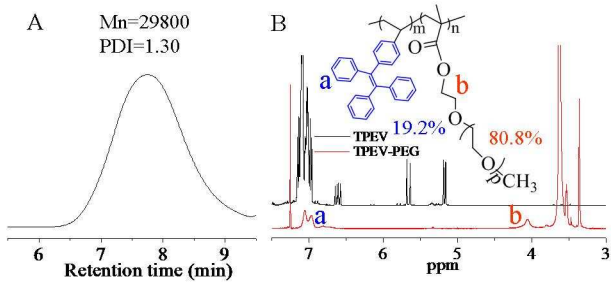

Fig. 1 (A) The GPC trace of TPEV-PEG (in DMF); (B) ^1H NMR spectra ($CDCl_3$) of TPEV fluorescent dye (black line) and the final obtained fluorescent copolymer TPEV-PEG (red line).

The characterization informations including TEM, UV, FL and FT-IR of the prepared TPEV dye and TPEV-PEG FONs were further described in Fig. 2. Transmission electron microscopy (TEM) of Fig. 2A indicates that TPEV-PEG copolymers tend to self-assemble into uniform spherical morphology with about 200 nm, which was further confirmed by DLS, and the results indicated that the size was also about 200 nm. The spherical morphology by self-assembly of the copolymers further confirms the successful incorporation of TPEV dye and PEGMA into the TPEV-PEG copolymers *via*

RAFT polymerization. The UV absorption spectrum of TPEV-PEG FONs water solution is displayed in Fig. 2B, and the absorption peaks present at 245 nm and 316 nm, which might be aroused by the electron transition of $\pi \rightarrow \pi^*$. The light transmission of nanoparticle will be effectively reduced by the light scattering or Mie effect, resulting in the apparent high absorption and levelling-off of the tail in the visible region.[32] It is clear that no absorption in the entire spectrum is discovered until the wavelength is below 390 nm, which is different with our previous result,[33] indicating the excellent water dispersibility of TPEV-PEG copolymers. The surface of TPEV-PEG FONs is encapsulated by hydrophilic PEG to form PEGylated AIE-based structure, which will endow the TPEV-PEG copolymers with the amphiphilic properties, making them tend to self-assemble into nanoparticles with the excellent water dispersibility. Fig. 2C demonstrates the fluorescence property of the obtained TPEV-PEG copolymers. From the fluorescence curve, the maximal emission peak at 480 nm is observed in the water solution, but almost no fluorescence is observed in the THF solution, implying obvious AIE property. The hydrophobic TPEV AIE dye can not dissolve in water but some organic solvent, so the obtained TPEV-PEG copolymers have better dissolution in some organic solvent than in water solvent. It is common for some compounds to be observed the AIE phenomenon, but the reason still remain unclear. A possible explanation for the AIE phenomenon is that the solute will aggregate into two kinds of nanoparticle suspensions: crystal particles and amorphous particles. The former will enhance the fluorescent intensity with shorter emission wavelength, but the latter will reduce the intensity with longer emission wavelength. The TPEV dye in the copolymers will exist as more crystalline state in water solution but more amorphous state in THF solution.[32, 34] Another possible explanation is that the intramolecular rotation is active in some organic solutions, serving as a relaxation avenue for the excited state to decay, while the rotation is restricted in the aggregation state due to the physical constraint, which blocks the non-radiative path and activates the radiative decay.[35]

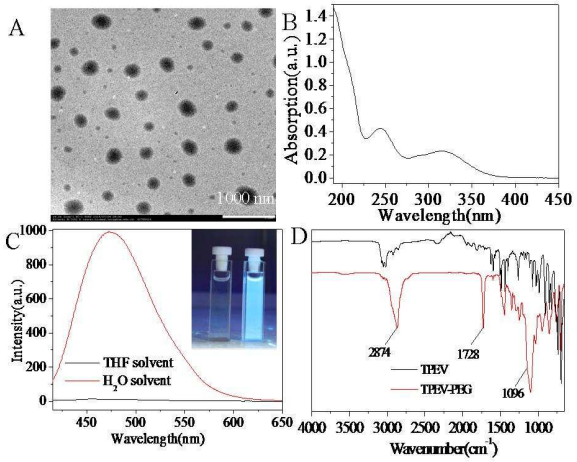

Fig. 2 Characterization of TPEV and TPEV-PEG FONs: (A) TEM image of TPEV-PEG FONs dispersed in water, scale bar=1000 nm; (B) UV-Vis spectrum of TPEV-PEG dispersed in water; (C) Fluorescence emission spectra of TPEV-PEG FONs in THF (left cuvette) and water (right cuvette), inset is the fluorescent image of TPEV-PEG FONs taken at 365 nm UV light; (D) FT-IR spectra of TPEV (black line) and TPEV-PEG (red line).

The FT-IR spectra of TPEV dye and TPEV-PEG copolymers are further described as shown in Fig. 2D. For the TPEV spectrum, the stretching vibration of the polycyclic aromatic rings locates at the range of 1380 to 1540 cm^{-1} with a series of absorbance peaks, and the peaks at 3020~3070 cm^{-1} should assign to the C-H stretching vibration of polycyclic aromatic. Moreover, two characteristic peaks locating at 1600 and 1630 cm^{-1} are aroused by the stretching vibration of C=C and CH_2=CH- bonds. For the spectrum of TPEV-PEG copolymers, the peak of -CH_2-, -CH_3 and polycyclic aromatic rings can also be clearly observed at 2874 cm^{-1} and the characteristic peaks of C=O stretching vibration peak is observed at 1740 cm^{-1}. As compared with the TPEV spectrum, the peak locating at 1630 cm^{-1} of CH_2=CH- bond is almost disappeared, indicating the successful incorporation of TPEV dye into the TPEV-PEG copolymers *via* RAFT polymerization. Otherwise, the spectrum presents one characteristic peak of C-O stretching vibration at 1100 cm^{-1}, which also confirms the successful incorporation of PEGMA into the copolymers by RAFT polymerization.

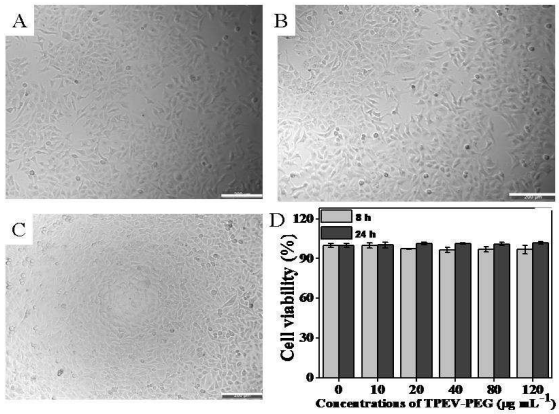

Fig. 3 Biocompatibility evaluations of TPEV-PEG FONs. (A–C) optical microscopy images of HepG2 cells incubated with different concentrations of TPEV-PEG FONs for 24 h, (A) control cells, (B) 20 μg mL^{-1}, (C) 80 μg mL^{-1}, (D) cell viability of TPEV-PEG FONs with HepG2 cells. The biocompatibility evaluation suggested that TPEV-PEG FONs were biocompatible enough for biomedical applications. Scale bar=200 μm.

The observation of cell morphology was used to investigate the biocompatibility of TPEV-PEG FONs with HepG2 cells when they were incubated with different concentrations of TPEV-PEG FONs for 24 h as shown in Fig. 3,[36-39] and the cell viability of TPEV-PEG FONs on HepG2 cells by the cell counting kit-8 (CCK-8) assay was also examined through the absorbance value of formazan dye at 450 nm with 620 nm as the reference wavelength.[40-41] Optical microscopy observations (Fig. 3A-C) indicated that cells maintained their normal morphology after they were incubated with different concentrations of TPEV-PEG FONs. No obvious cell morphology change could be observed even when the concentration of TPEV-PEG FONs was increased to 80 mg mL^{-1}. To further confirm the good biocompatibility of TPEV-PEG FONs, the cell viability of TPEV-PEG FONs with HepG2 cells was determined by cell counting kit-8 (CCK-8) assay as shown in Fig. 3D,[42-44] and the results demonstrated that it wasn't obvious for the decrease of cell viability to be observed when the cells were incubated with 10-120 mg mL^{-1} of TPEV-PEG FONs. Even when the concentration was as high as 120 mg mL^{-1}, the cell viability values were still more than 90%. From the

above results, it was confirmed that TPEV-PEG FONs had good biocompatibility and were highly potential for biomedical applications.

Considering the high water dispersibility, good fluorescence and excellent biocompatibility of the TPEV-PEG copolymers, their potential applications in cell imaging together with the cell uptake effect was further investigated by confocal laser scanning microscopy (CLSM) as shown in Fig. 4 after they were uptaken by HepG2 cells.[34, 45-46] The bright dots were the HepG2 cells, and the presence of the obvious blue fluorescence implied that the TPEV-PEG FONs have been uptaken by HepG2 cells. With careful observation, the TPEV-PEG FONs mainly located at the cytoplasm, and the centre areas of the dots with relatively weak fluorescence intensity should be the cell nuclei (Fig. 4B).[11] From the above preliminary results, it was concluded that TPEV-PEG FONs could be easily internalized by cells with most of them locating at the cytoplasm. Considering the size of TPEV-PEG FONs and nucleus pore, it was possible for these FONs to be taken up by endocytosis of the cells.[47] Combining the merits of AIE and PEG with good fluorescent feature, high water dispersibility and excellent biocompatibility, the obtained TPEV-PEG FONs were considered to be biocompatible enough for bioimaging applications. Finally, in consideration of the controllability of RAFT polymerization, other polymerizable AIE dyes with different optical properties and numerous monomers with different functional groups could also be easily incorporated into FONs polymer, thus, it was expected for the multifunctional imaging and theranostic platforms to be obtained by controllable polymerization of polymerizable AIE dyes and some multifunctional monomers.

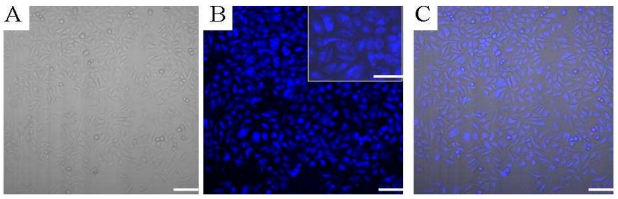

Fig. 4 CLSM images of HepG2 cells incubated with 80 μg mL^{-1} of TPEV-PEG FONs. (A) bright field, (B) excited with a 405 nm laser (inset is the local zoom, scale bar=50 μm), (C) merged image of (A) and (B). Scale bar = 100 μm.

4. Conclusions

In summary, we synthesized a hydrophobic TPEV AIE dye with a vinyl end functional group by "one-step" Suzuki coupling reaction of 4-vinylphenylboronic acid and bromotriphenylethylene with high yield, which subsequently participated in RAFT polymerization with a widely used biomedical molecule (PEGMA) monomers to obtain the TPEV-PEG copolymers with the transformed side fluorescent groups. The M_n value of the obtained copolymer was about 29800 g mol^{-1} with a narrow PDI as about 1.30, and the molar fraction of hydrophobic TPEV dye and hydrophilic PEG segment in the copolymer was calculated as about 19.2% and 80.8% on the basis of the ^{1}H NMR spectrum, respectively. The as-prepared amphiphilic TPEV-PEG copolymers tended to self-assemble into stable FONs in aqueous solution, with the hydrophobic AIE core coved by hydrophilic PEG shell. Moreover, in consideration of the favourable properties of TPEV-PEG FONs with high water dispersibility, bright fluorescence and excellent biocompatibility, it was promising for them to be applied in bioimaging field. In view of the controllability of RAFT polymerization, various polymerizable AIE dye can also incorporate into polymer through RAFT polymerization to prepare multifunctional FONs, which is very important for the construction of multifunctional theranostics systems. It was concluded that RAFT polymerization by employing various polymerizable AIE dyes should be a facile and efficient strategy for the fabrication of multifunctional AIE-based FONs with other components, such as targeting agents, drugs, genes or other imaging agents, and these FONs are expected to show great potential for various biomedical applications.

Acknowledgements

This research was supported by the National Science Foundation of China (Nos. 21474057, 21104039, 21134004, 51363016), and the National 973 Project (Nos. 2011CB935700), the Natural Science Foundation of Guangdong Province (S2013010013580)

References

1 D. Quémener, T. Davis, C. Barner-Kowollik and M. Stenzel, *Chem. Commun.*, 2006, **42**, 5051-5053.
2 M. Kade, D. Burke and C. Hawker, *J. Polym. Sci., Part A: Polym. Chem.*, 2010, **48**, 743−750.
3 H. Li, B. Yu, H. Matsushima, C. Hoyle and A. Lowe, *Macromolecules*, 2009, **42**, 6537-6542.
4 C. Becer, R. Hoogenboom and U. Schubert, *Angew. Chem., Int. Ed.*, 2009, **48**, 4900-4908.
5 M. Li, P. De, S. Gondi and B. Sumerlin, *Macromol. Rapid Commun.*, 2008, **29**, 1172-1176.
6 C. Boyer, V. Bulmus, T. Davis, V. Ladmiral, J. Liu and S. Perrier, *Chem. Rev.* 2009, **109**, 5402-5436.
7 S. Perrier and P. Takolpuckdee, *J. Polym. Sci., Part A: Polym. Chem.*, 2005, **43**, 5347-5393.
8 S. Wang, C. Fu, Y. Zhang, L. Tao, S. Li and Y. Wei, *ACS Macro. Lett.*, 2012, **1**, 1224-1227.
9 Y. Zhang, Y. Zhao, B. Yang, C. Zhu, Y. Wei and L. Tao, *Polym. Chem.*, 2014, **5**, 1857–1862.
10 X. Shen, Y. Shi, B. Peng, K. Li, J. Xiang, G. Zhang, Z. Liu, Y. Chen and D. Zhang, *Macromol. Biosci.*, 2012, **12**, 1583-1590.
11 X. Zhang, M. Liu, B. Yang, X. Zhang, Z. Chi, S. Liu, J. Xu, and Y. Wei, *Polym. Chem.*, 2013, **4**, 5060-5064.
12 X. Zhang, X. Zhang, B. Yang, J. Hui, M. Liu, W. Liu, Y. Chen and Y. Wei, *Polym. Chem.*, 2014, **5**, 689-693.
13 X. Zhang, X. Zhang, B. Yang, J. Hui, M. Liu, Z. Chi, S. Liu, J. Xu and Y. Wei, *Polym. Chem.*, 2014, **5**, 683-688.
14 X. Zhang, X. Zhang, L. Tao, Z. Chi, J. Xu and Y. Wei, *J. Mater. Chem. B*, 2014, **2**, 4398-4414.
15 H. Tong, Y. Hong, Y. Dong, Y. Ren, M. Haeussler, J. Lam, K. Wong and B. Tang, *J. Phys. Chem. B*, 2007, **111**, 2000-2007.
16 H. Tong, Y. Dong, Y. Hong, M. Haeussler, J. Lam, H. Sung, X. Yu, J. Sun, I. Williams, H. Kwok and B. Tang, *J. Phys. Chem. C*, 2007, **111**, 2287-2294.
17 R. Hu, N. Leung and B. Tang, *Chem. Soc. Rev.,* 2014, **43**, 4494-4562.
18 X. Zhang, Z. Chi, H. Li, B. Xu, X. Li, W. Zhou, S. Liu, Y. Zhang and J. Xu, *Chem.- Asian J.*, 2011, **6**, 808-811.
19 X. Zhang, Z. Chi, H. Li, B. Xu, X. Li, S. Liu, Y. Zhang and J. Xu, *J. Mater. Chem.*, 2011, **21**, 1788-1796.
20 X. Zhang, Z. Chi, B. Xu, C. Chen, X. Zhou, Y. Zhang, S. Liu and J. Xu, *J. Mater. Chem.*, 2012, **22**, 18505-18513.
21 J. Liu, J. Lam and B. Tang, *J. Inorg. Organomet. Polym.*, 2009, **19**, 249-285.

22 J. Liu, J. Lam and B. Tang, *Chem. Rev.*, 2009, **109**, 5799-5867.
23 L. Tang, J. Jin, A. Qin, W. Yuan, Y. Mao, J. Mei, J. Sun and B. Z. Tang, *Chem. Commun.*, 2009, **45**, 4974-4976.
24 R. Hu, J. Maldonado, M. Rodriguez, C. Deng, C. Jim, J. Lam, M. Yuen, G. Ramos-Ortiz and B. Tang, *J. Mater. Chem.*, 2012, **22**, 232-240.
25 R. Hu, J. Lam, Y. Yu, H. Sung, I. Williams, M. Yuen and B. Tang, *Polym. Chem.*, 2013, **4**, 95-105.
26 X. Zhang, M. Liu, B. Yang, X. Zhang and Y. Wei, *Colloids and Surfaces B: Biointerfaces*, 2013, **112**, 81-86.
27 Z. Huang, X. Zhang, X. Zhang, C. Fu, K. Wang, J. Yuan, L. Tao and Y. Wei, *Polym. Chem.*, 2015, **6**, 607-612.
28 L. Tao, J. Liu and T. Davis, *Biomacromolecules*, 2009, **10**, 2847-2851.
29 Z. Huang, X. Zhang, X. Zhang, S. Wang, B. Yang, K. Wang, J. Yuan, L. Tao and Y. Wei，*RSC Adv.*, 2015, **5**, 65884–65889.
30 Z. Huang, X. Zhang, X. Zhang, B. Yang, Y. Zhang, K. Wang, J. Yuan, L. Tao, Y. Wei, *Polym. Chem.*, 2015, **6**, 2133-2138.
31 D. Jana and B. Ghorai, Tetrahedron Lett. 2012, **53**, 196-199.
32 X. Zhang, Z. Chi, J. Zhang, H. Li, B. Xu, X. Li, S. Liu, Y. Zhang and J. Xu, *J. Phys. Chem. B*, 2011, **115**, 7606-7611.
33 X. Zhang, X. Zhang, B. Yang, J. Hui, M. Liu, Z. Chi, S. Liu, J. Xu and Y. Wei, *Polym. Chem.*, 2014, **5**, 318-322.
34 X. Zhang, X. Zhang, B. Yang, M. Liu, W. Liu, Y. Chen and Y. Wei, *Polym. Chem.*, 2014, **5**, 356-360.
35 Y. Hong, J. Lam and B. Tang, *Chem. Commun.*, 2009, **45**, 4332-4353.
36 X. Zhang, J. Yin, C. Peng, W. Hu, Z. Zhu, W. Li, C. Fan and Q. Huang, *Carbon*, 2011, **49**, 986-995.
37 X. Zhang, S. Wang, C. Zhu, M. Liu, Y. Ji, L. Feng, L. Tao and Y. Wei, *J. Colloid Interf. Sci.*, 2013, **397**, 39-44.
38 X. Zhang, X. Zhang, S. Wang, M. Liu, L. Tao and Y. Wei, *Nanoscale*, 2013, **5**, 147-150.
39 X. Zhang, W. Hu, J. Li, L. Tao and Y. Wei, *Toxicol. Res.*, 2012, **1**, 62-68.
40 X. Zhang, H. Qi, S. Wang, L. Feng, Y. Ji, L. Tao, S. Li and Y. Wei, *Toxicol. Res.*, 2012, **1**, 201-205.
41 X. Zhang, J. Hui, B. Yang, Y. Yang, D. Fan, M. Liu, L. Tao and Y. Wei, *Polym. Chem.*, 2013, **4**, 4120-4125.
42 H. Qi, M. Liu, L. Xu, L. Feng, L. Tao, Y. Ji, X. Zhang and Y. Wei, *Toxicol. Res.*, 2013, **2**, 427-433.
43 X. Zhang, S. Wang, M. Liu, J. Hui, B. Yang, L. Tao and Y. Wei, *Toxicol. Res.*, 2013, **2**, 335-346.
44 K. Wang, X. Zhang, X. Zhang, B. Yang, Z. Li , Q. Zhang , Z. Huang and Y. Wei, *Macromol. Chem. Phys.*, 2015, **216**, 678-684.
45 B. Yang, Y. Zhang, X. Zhang, L. Tao, S. Li and Y. Wei, *Polym. Chem.*, 2012, **3**, 3235-3238.
46 X. Zhang, S. Wang, C. Fu, L. Feng, Y. Ji, L. Tao, S. Li and Y. Wei, *Polym. Chem.*, 2012, **3**, 2716-2719.
47 H. Li, X. Zhang, X. Zhang, B. Yang, Y. Yang and Y. Wei, *Polym. Chem.*, 2014, **5**, 3758-3762.